Journal of Food Engineering 125 (2014) 147–156

Contents lists available at ScienceDirect

Journal of Food Engineering

journal homepage: www.elsevier.com/locate/jfoodeng

Parameter estimation applied to the heat transfer characterisation of Scraped Surface Heat Exchangers for food applications

S. Rainieri [a,b,*], F. Bozzoli [a], L. Cattani [a], P. Vocale [a]

[a] Department of Industrial Engineering, University of Parma, Parco Area delle Scienze 181/A, I-43124 Parma, Italy
[b] SITEIA.PARMA Interdepartmental Centre, University of Parma, Parco Area delle Scienze 181/A, I-43124 Parma, Italy

ARTICLE INFO

Article history:
Received 5 March 2013
Received in revised form 14 October 2013
Accepted 21 October 2013
Available online 30 October 2013

Keywords:
Parameter estimation
Sensitivity and uncertainty analysis
Scraped Surface Heat Exchangers
Highly viscous food product

ABSTRACT

A parameter estimation approach was applied to characterise the heat transfer of Scraped Surface Heat Exchangers (SSHEs) specifically designed for the food industry. It is difficult to apply the data available in the literature to SSHEs, due to the specificity of each product, thermal treatment and geometrical configuration, making the thermal design of these apparatuses critical. Therefore, it appears to be more useful to assess the methodology used to derive a proper heat transfer correlation than to assess the form of the heat transfer correlation itself, as the correlation often cannot be transferred to other heat exchangers, even those that belong to the same class.

This study enabled successful and robust estimation of the heat transfer correlation for the product side Nusselt number and the external side heat transfer coefficient; this approach differs from Wilson plot methods, as no assumption is made regarding the functional dependence of the external side heat transfer coefficient.

The procedure was validated through application to both synthetic data and experimental data acquired from a coaxial SSHE pilot plant for the treatment of highly viscous fluid foods.

The procedure was optimised with the aid of sensitivity and uncertainty analysis, which provided considerable insight into the problem.

The application to synthetic data demonstrated that under typical operating conditions, areas of insensitivity to certain parameters are present. The application to the experimental data acquired under both heating and cooling conditions confirmed that the measured values of the overall heat transfer coefficient can be used to estimate the secondary fluid heat transfer coefficient, as well as the power law dependence of the internal fluid Nusselt number on the rotational Reynolds number and the Prandtl number together with the multiplicative constant. The uncertainty analysis provided the confidence intervals associated with each estimated parameter, thereby enabling the quality and robustness of the resulting heat transfer correlations to be determined.

1. Introduction

Parameter estimation represents a powerful tool for many engineering applications such as the design of heat exchangers. In fact, this approach offers the ability to estimate unknown parameters, which are often crucial for the design and optimisation of the whole heat transfer apparatus. This strategy appears to be particularly useful in the design of heat exchangers that are customised for certain specific purpose, as often happens with Scraped Surface Heat Exchangers (SSHEs). SSHEs may provide a suitable solution to actively enhance the convective heat transfer mechanism in highly viscous or sticky fluids, i.e., in conditions that are generally critical due to the limited heat transfer coefficients that can be achieved given the low Reynolds number values that generally characterise the fluid flow, as shown by Bozzoli et al. (2010), Rainieri et al. (2011, 2012a, 2013), Datta (2002) and Rozzi et al. (2007).

In these heat exchangers, the product to be heated/cooled flows axially in an annular section between a stationary outer cylinder and a powered coaxial rotor. The inner wall of the outer cylinder is periodically scraped by blades attached to the rotor, while the heating or cooling fluid circulates into the external jacket, which is generally equipped with flow baffles.

There are generally between two and four blades, which can be arranged longitudinally on the rotor wall along the whole length of the heat exchanger. Alternatively, short blades can be arranged in couples and shifted by 180° with respect to the rotor axis, in the presence or absence of some degree of overlap. These two

* Corresponding author at: Department of Industrial Engineering, University of Parma, Parco Area delle Scienze 181/A, I-43124 Parma, Italy. Tel.: +39 0521 905857; fax: +39 0521 905705.

E-mail address: sara.rainieri@unipr.it (S. Rainieri).

0260-8774/$ - see front matter © 2013 Elsevier Ltd. All rights reserved.
http://dx.doi.org/10.1016/j.jfoodeng.2013.10.031

Nomenclature

A_i	heat transfer inner surface area, $A_i = \pi D_i L$ (m^2)
A_o	heat transfer outer surface area, $A_o = \pi D_o L$ (m^2)
C	multiplicative constant, Eq. (6)
$CI^{95\%}$	confidence interval, Eq. (14)
CV	coefficient of variation, Eq. (15)
D_i	exchanger tube inner diameter (m)
D_o	exchanger tube outer diameter (m)
D_r	rotor shaft diameter (m)
h	convective heat transfer coefficient (W/m^2 K)
j	fluid specific enthalpy (J/kg)
J^*	scaled sensitivity coefficient
$\mathbf{J}$	Jacobian operator
L	heat exchanger's length (m)
m	mass flow rate (kg/s)
n	number of blades
N	rotational velocity (r.p.s)
Nu	inner side Nusselt number, Eq. (5)
P_i	generic unknown parameter
Pr	Prandtl number
Q	heat transfer rate (W)
R_w	wall thermal resistance (K/W)
Re_r	rotational Reynolds number, Eq. (7)
S	target function
T	fluid temperature (K, °C)
U	overall heat transfer coefficient (W/m^2·K)
α	Reynolds number exponent, Eq. (6)
β	Prandtl number exponent, Eq. (6)
ΔT_{ml}	logarithmic mean temperature difference (K, °C)
η	fluid dynamic viscosity (Pa s)
λ	fluid thermal conductivity (W/m K)
λ_w	wall thermal conductivity (W/m K)
ρ	density (kg/m^3)
σ	standard error

Subscripts

i	inner-side
o	outer-side
in	inlet section
out	outlet section

configurations are named continuous and alternate blades, respectively (D'Addio et al., 2012).

In any of the possible configurations, the heat transfer coefficient is augmented by the mixing of the fluid in the boundary layer, activated by the rotation of the shaft (Härröd, 1986) and by backmixing phenomena (D'Addio et al., 2013). The complex flow pattern established in SSHEs is often described by adopting the axial Reynolds number and the rotational Reynolds number (Härröd, 1986).

Increasing the rotational Reynolds number results in several different flow regimes (Härröd, 1986), and this complex flow is affected by many factors including the blade profile, the entry region effect, the possible non-Newtonian rheological behaviour and the thermally induced modification of the working fluid properties.

Although SSHEs are frequently used in industrial applications such as in the dairy and food industry where the fluid under treatment often undergoes phase changes and is often highly viscous and exhibits complex rheological behaviour, the scientific literature on this topic contains some gaps, including the thermal design of these apparatuses (Boccardi et al., 2010; Fayolle et al., 2013). Very few studies in the open scientific literature address the topic of SSHE design using a theoretical approach (Härröd, 1986), although the numerical approach has led to some critical results (Yataghene and Legrand, 2013; Rainieri et al., 2012b).

Most studies about SSHEs are based on experimental investigations of single-phase and two-phase heat transfer modalities. The mostly widely used correlations have been reviewed by Härröd (1986), Abichandani and Sarma (1987) and Skelland (1958).

The experimental data are treated by adopting the dimensional analysis approach, but due to the specificity of each plant and product treated, it is often difficult to extend the validity of the suggested heat transfer correlations that often hold for the particular geometry under investigation.

Generally, the experimental investigations reported in the literature aim to measure the average product Nusselt number for different conditions (different rotational or axial Reynolds number values, heating/cooling conditions) and different geometric configurations (number and/or profile of the blades). The product convective heat transfer coefficient is generally indirectly derived by measuring the overall heat transfer coefficient, which accounts for both the internal and external convection thermal resistances, and for the conductive thermal resistance of the tube wall. This procedure is sometimes performed by assuming that the external thermal resistance is much lower than the inner resistance (D'Addio et al., 2013). This simplified approach can lead to misleading conclusions for SSHEs because increasing the rotational velocity of the rotor makes the magnitude of the inner and outer thermal resistances comparable.

For the internal side heat transfer correlation, a monomial form is generally adopted by accounting for the dependence of the Nusselt number on the rotational Reynolds number and the Prandtl number, while the dependence on the axial Reynolds number is generally disregarded (Härröd, 1986).

One of the simplest methods used to account for the external side heat transfer coefficient is the well-known Wilson plot technique (Wilson, 1915), which was originally developed to estimate the inside heat transfer coefficient in a steam condenser by holding the shell side mass flow rate constant and assuming a known power law dependence of the internal heat transfer coefficient on the fluid velocity (Wilson, 1915). A simple linear curve fitting procedure was used to estimate both the sum of the wall and shell side resistances and the constant of the internal side heat transfer correlation. Briggs and Young (1969) suggested and validated a procedure for determining three unknowns rather than two, as the exponent expressing the power law dependence of the internal Nusselt number on the Reynolds number was also estimated. A more general approach based on a non-linear regression scheme was presented by Khartabil and Christensen (1992). A unified Wilson plot method based on non-linear regression was applied by Styrylska and Lechowska (2003). Some of these approaches assume that the external side heat transfer is constant, while others assume that it follows some specific correlation, the parameters of which have to be estimated.

A general review of the Wilson plot method and its modifications to determine convection coefficients in heat exchanger devices is presented by Rose (2004) and Fernández-Seara et al. (2007).

In our opinion, this approach appears to be unsuitable to accurately describe the performance of SSHEs. In fact, the convective heat transfer on the external side cannot often be analytically determined with enough accuracy because the geometry of the external jacket is often more complex than a simple annular channel, and also because baffles of different shapes and inclinations are generally used to improve mixing or promote turbulence. In this case, parameter estimation procedures can provide a valid strategy to extract the convective heat transfer coefficients from the measured values of the overall heat transfer coefficient.

While the Wilson plot method and its subsequent modifications have been applied to several types of heat exchangers such as tube-in-tube or shell and tube heat exchangers, and also to cases of two phase heat transfer (Rose, 2004; Fernández-Seara et al., 2007), to our knowledge the application of parameter estimation procedures to SSHEs has not yet been deeply investigated in the literature.

The present work reports the application of a data processing procedure based on the parameter estimation methodology to the characterisation of SSHEs. This investigation is intended to enable the robust estimation of the heat transfer correlation for the product side Nusselt number by assuming unknown the external side heat transfer coefficient and by assuming it variable with the secondary fluid mass flow rate. This approach differs from both the original and the modified Wilson plot methods in that no assumption is made regarding the functional dependence of the external side heat transfer coefficient.

Moreover, the uncertainty analysis is complex for Wilson plot techniques (Uhia et al., 2013), and therefore it is often overlooked. However, in our opinion, parameter estimation cannot be addressed without considering uncertainty, and the estimated parameter values are not fully useful without reporting the associated confidence interval. For this reason, the parameter estimation procedure reported here was optimised with the aid of the sensitivity and uncertainty analyses, both of which provided considerable insight into the problem by enabling an assessment of the quality and robustness of the resulting heat transfer correlations.

The procedure was validated through its application to both synthetic data and experimental data acquired from a coaxial SSHE pilot plant. In particular, the highly viscous fluid glycerol was tested as a working fluid over rotational Reynolds numbers ranging from 50 to 700. The experimental conditions have been tailored to simulate the actual operating conditions under which SSHEs are used in the food industry.

2. Parameter estimation and sensitivity analysis for the characterisation of SSHE behaviour

For any parallel flow heat exchanger, the average overall heat transfer coefficient U for the inner heat transfer surface area A_i can be obtained from the equation:

$$U = \frac{Q}{A_i \Delta T_{ml}} \tag{1}$$

where ΔT_{ml} is the logarithmic mean temperature difference and Q is the heat flow rate. This definition is based on the following hypothesis:

1. the steady state condition is verified;
2. the heat exchanger is perfectly thermally insulated from the environment;
3. the heat conduction in the flow direction is negligible.

For realistic applications, SSHEs only partially meet the assumptions stated above, furthermore the parallel flow condition is verified only by the average flow; however, the definition of the overall heat transfer coefficient given by Eq. (1) is commonly accepted and adopted to evaluate the thermal performance of this type of equipment (Geankoplis, 2003). Moreover, the error introduced by using Eq. (1) is often negligible in comparison to the measurement chain error.

In Eq. (1), the heat flow rate Q can be recovered by determining the energy balance of the secondary fluid stream flowing in the jacket side as follows:

$$Q = m_o(j_{o,out} - j_{o,in}) \tag{2}$$

where $j_{o,out}$ and $j_{o,in}$ express the outer-side fluid specific enthalpy evaluated at the outlet and inlet sections, respectively.

The energy balance could also be evaluated for the product fluid stream, but in this case, some care is needed in the measurement of the bulk temperature, as a fluid thermal stratification is expected to occur over the cross section, and moreover the contribution of the dissipated work due to the rotating element has to be accounted for. The overall heat transfer coefficient is related to the product side and secondary fluid convective heat transfer coefficients by the following equation:

$$\frac{1}{UA_i} = \frac{1}{h_i A_i} + R_w + \frac{1}{h_o A_o} \tag{3}$$

where h_i is the convective heat transfer coefficient of the product flowing in the tube equipped with the rotor and h_o is the convective heat transfer coefficient of the fluid stream flowing in the jacket side, A_i and A_o are the inner and outer heat transfer surface areas and R_w is the thermal resistance of the wall that separates the two fluids, expressed as follows:

$$R_w = \frac{\ln(D_o/D_i)}{2\pi\lambda_w L} \tag{4}$$

where λ_w is the thermal conductivity of the wall material and L is the length of the heat exchanger.

The wall thermal resistance R_w can be assumed to be known and constant for a given heat exchanger under a given operating condition.

Using the exchanger tube's internal diameter as the characteristic length, the internal side Nusselt number is expressed in the following straightforward manner:

$$Nu = \frac{h_i D_i}{\lambda} \tag{5}$$

where λ is the product (inner side fluid) thermal conductivity.

It is difficult to predict which thermal resistance in Eq. (3) is dominant for SSHEs, as variations in the rotational velocity of the rotor may induce significant variations of the internal-side heat transfer coefficient.

In Eq. (3), both h_i and h_o are generally unknown, and can be determined with suitable accuracy by adopting a parameter estimation technique under an inverse problem data processing methodology (Beck and Arnold, 1977).

With regard to SSHEs, under the hypothesis of single-phase flow, the product side heat transfer coefficient can be assumed to be correlated in terms of the Nusselt number as follows:

$$Nu = CRe_r^{\alpha} Pr^{\beta} \tag{6}$$

where the rotational Reynolds number Re_r is defined according to Härröd (1986) as follows:

$$Re_r = \frac{N(D_i)^2 \rho}{\eta} \tag{7}$$

In Eq. (7), N is the rotational velocity and η and ρ are the product dynamic viscosity and density, respectively.

For the outer-side heat transfer coefficient, it is difficult to identify a heat transfer correlation because the jacket side generally has a complex geometrical configuration that can modify the flow regime in unpredictable ways. Therefore, the value of the outer-side convective heat transfer coefficient has to be considered an unknown parameter. Moreover, under typical operating conditions, the external side heat transfer coefficient can be considered to depend on the fluid mass flow rate only, as the service fluid temperature often undergoes small changes (Fernández-Seara et al., 2007).

Therefore, an SSHE can be described by assuming that the unknown variables in Eqs. (3) and (6) are C, α, β, and h_o, with this last parameter assumed to vary with the secondary fluid mass flow rate. In principle, these variables could be concurrently estimated by the parameter estimation approach by minimising the squared errors of the prediction with respect to the experimentally measured values for U (Beck and Arnold, 1977).

This implies that the following function should be minimised using the usual least squares approach:

$$S(h_o, C, \alpha, \beta) = \sum_{j=1}^{M} [U_{\exp,j} - U_{calc,j}]^2 \tag{8}$$

where M is the number of measurements made for a given secondary fluid mass flow rate by varying Re_r and Pr, with the resulting U_{calc} expressed as follows:

$$U_{calc} = \frac{1}{A_i}\left(\frac{D_i}{A_i \lambda C Re_r^{\alpha} Pr^{\beta}} + R_w + \frac{1}{A_o h_o}\right)^{-1} \tag{9}$$

Then, the parameter estimation procedure applied to the heat transfer characterisation of SSHEs results in the minimisation of the objective function S given by Eq. (8) by assuming Re_r and Pr as the independent variables; C, α, β and h_o as the unknown variables, and all the other properties and geometrical quantities as known.

The practical possibility of concurrently estimating all the unknown parameters (C, α, β and h_o) is only feasible if the parameter sensitivity coefficients for the output variable U with respect to each parameter are linearly independent over the range of interest (Beck and Arnold, 1977). In practice, the sensitivity coefficients quantify the extent to which variations in the parameters of interest affect the output of the system, which is evaluated in the present case by measuring the overall heat transfer coefficient U. The coefficients are then defined with respect to the generic parameter P_i in a dimensionless form as follows:

$$J_i^* = \frac{1}{U}\frac{\partial U}{\partial P_i} P_i \tag{10}$$

where P_i represents the unknown variables, i.e., C, α, β and h_o, and U is the overall heat transfer coefficient expressed as a function of the independent variables Re_r and Pr.

Although the sensitivity analysis is a useful tool to theoretically verify the possibility of concurrently estimating several unknown variables, it does not provide any quantitative information about the uncertainty associated with each estimated value (Blackwell and Beck, 2010). A well-known method used to address this issue involves the computation of confidence intervals for the parameter estimates using asymptotic theory (Banks et al., 2010; Seber and Wild, 2003). Following this approach, once the optimal curve-fit parameters $\mathbf{P}$ are determined, the parameter standard errors $\boldsymbol{\sigma}_P$ are given by:

$$\boldsymbol{\sigma}_P = \sqrt{\sigma_U^2 \cdot diag([\mathbf{J}^T \cdot \mathbf{J}]^{-1})} \tag{11}$$

where $\mathbf{J}$ is the Jacobian matrix of the target variable, i.e., the function U_{calc}

$$\mathbf{J} = \left[\frac{\partial \mathbf{U}_{calc}(\mathbf{P})}{\partial \mathbf{P}}\right] \tag{12}$$

and σ_U^2 is the residual variance:

$$\sigma_U^2 = \frac{1}{M - z}\sum_{j=1}^{M}[U_{\exp,j} - U_{calc,j}(\mathbf{P})] \tag{13}$$

where M is the number of measurements and z is the number of parameters to be fitted.

In order to express the reliability of the parameter estimates and to compare the relative precision of different parameter estimates the 95% confidence interval, $CI^{95\%}$, and the coefficient of variation, CV, are generally used (Banks et al., 2010). With regard to the parameter P_i, they are defined as follows:

$$CI_{P_i}^{95\%} = (P_i - 1.96\sigma_{Pi}, P_i + 1.96\sigma_{Pi}) \tag{14}$$

$$CV_{P_i} = \frac{\sigma_{Pi}}{P_i} \tag{15}$$

The sensitivity and uncertainty analyses were applied to both synthetic and experimental data for a coaxial SSHE.

It must be stressed that the approach presented here, based on the assumption that the external side heat transfer coefficient varies with the secondary fluid mass flow rate, is optimised for apparatuses in which single-phase convection is present on the secondary fluid side. If evaporation or condensation occur in the external jacket, then this method should be applied with caution because other terms apart from the fluid mass flow rate drive the mechanism of heat transfer (e.g., vapour quality, heat flux, and pressure).

3. Application of the parameter estimation approach to synthetic data

To test the parameter estimation approach, the function given in Eq. (8) was minimised for synthetic data. The data sets were generated for an SSHE with $L = 2$ m, $R_w = 2.8 \cdot 10^{-4}$ K/W, $A_i = 0.93$ m^2, and $A_o = 0.98$ m^2 by varying Re_r over the range of 50–1000 and randomly varying Pr over the range of 1000–3000 and assuming that the values $\alpha = 0.76$, $\beta = 0.24$ and $C = 1.8$ are representative of the behaviour of a real SSHE (Härröd, 1986). The convective heat transfer coefficient of the fluid stream flowing in the jacket side, namely h_o, was first varied over the range 1000–4000 W/m^2 K, which is representative of SSHEs in which the secondary fluid flows under the turbulent regime, as often happens when water is used as the service fluid.

To verify the possibility of concurrently estimating the unknown parameters, i.e., h_o, C, α and β, it is important to analyse the behaviour and the relative magnitude of their sensitivity coefficients versus the independent variables, i.e., the rotational Reynolds number and the Prandtl number.

In Fig. 1(a) and (b), the scaled sensitivities are reported for a single Pr number value ($Pr = 2000$) versus the rotational Reynolds number for the representative cases: $C = 1.8$, $\alpha = 0.6$, $\beta = 0.24$, $h_o = 1000$ and 4000 W/m^2 K, respectively.

The trends of J_{ho}^*, J_C^* and J_α^* confirm that the concurrent estimation of the three parameters is feasible, although the relative magnitude of the three scaled sensitivities varies significantly with the progression of h_o. In particular, by increasing h_o, the low values assumed by J_{ho}^* suggest that it is critical to estimate the external heat transfer coefficient in this operating condition. This point, which ultimately arises due to the relative magnitudes of the thermal resistances, was also observed by Khartabil and Christensen (1992), who analysed the accuracy that could be achieved with

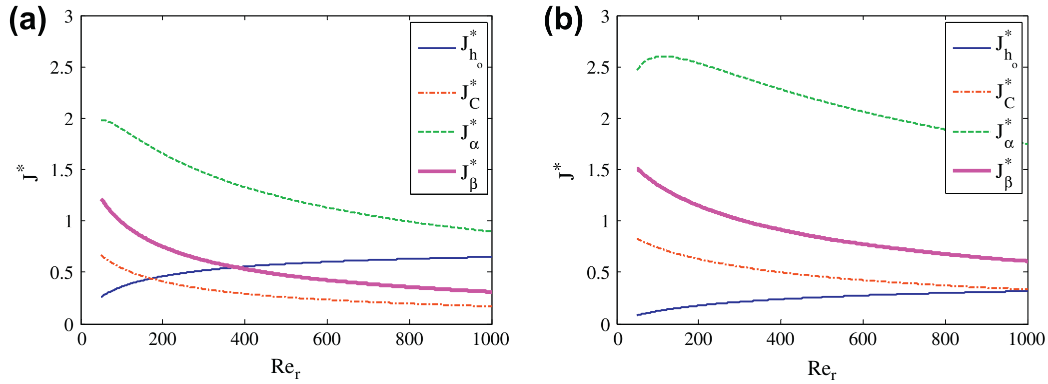

Fig. 1. Scaled sensitivity coefficients versus the Reynolds number for C = 1.8, α = 0.7, β = 0.24, Pr = 2000, with h_o = 1000 W/m^2 K (a) and h_o = 4000 W/m^2 K (b).

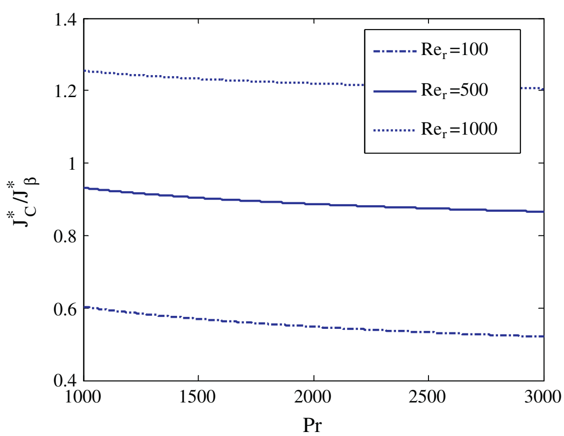

Fig. 2. Ratio between the scaled sensitivity coefficients of C and β versus the Prandtl number for C = 1.8, α = 0.7 and β = 0.24 for the case of h_o = 4000 W/m^2 K.

non-linear regression models in the characterisation of heat exchangers based on experimental measurements of the overall heat transfer coefficient. On the other hand, for the lowest h_o value considered here, the estimation of the multiplicative constant C is identified as the critical issue. Moreover, the presence of a maximum of J^*_α in the low rotational Reynolds number range suggests that the experimental conditions can be optimally designed to accurately infer the α exponent through the minimisation of the functional S.

Regarding the trend of J^*_β versus Re_r reported in Fig. 1(a) and (b), as expected, J^*_β shows a linear dependence on J^*_C for a given Pr value, with the multiplicative constant correlated with the Prandtl exponent. To make the estimation of the β exponent feasible independently from the multiplicative constant C, it is obviously necessary to consider a sensitivity analysis by assuming that the Prandtl number is the independent variable. Moreover, both C and β can be successfully estimated if they are linearly independent: this condition can be verified by evaluating the ratio J^*_C/J^*_β versus the Prandtl number (Beck and Arnold, 1977). This function is reported in Fig. 2 for three representative Reynolds number values in a Prandtl number range of interest for SSHE applications ($1000 < Pr < 3000$). The fact that the ratio J^*_C/J^*_β is not constant over the Prandtl number range considered here confirms the feasibility of independently estimating both the multiplicative constant and the Prandtl number exponent.

To identify a strategy to accurately determine the secondary fluid convective heat transfer coefficient h_o as well as α and C, it is necessary to perform various measurements characterised by different values of the external side thermal resistance to cover the space of possible values for the design variables.

To simulate the presence of experimental noise, multiplicative white noise with a mean of zero and a constant variance was superimposed to the overall heat transfer coefficient distributions as follows:

$$U_{exp} = U_{calc}(1+\varepsilon) \qquad (16)$$

where ε is the uniformly distributed random noise with zero mean and variance σ. Two different variance values were considered, σ = 1% and 5%. The synthetic U-data set is reported in Fig. 3 versus Re_r for the representative case σ = 1% by assuming four h_o values, namely $h_{o,1}$ = 1000, $h_{o,2}$ = 2000, $h_{o,3}$ = 3000 and $h_{o,4}$ = 4000 W/m^2 K, with Pr randomly distributed over the range 1000–3000.

At first, the estimation procedure was developed by separately considering each set of data characterised by a given h_o value. Therefore, the functional to be minimised was defined as follows:

$$S(h_{0,i}, C_i, \alpha_i, \beta_i) = \sum_{j=1}^{M} [U_{\exp,j} - U_{calc,j}]^2 \quad i = 1, 2, \ldots, K \qquad (17)$$

where K is the number of datasets, each containing M measurements.

To assess the robustness of the estimation approach, the functional given by Eq. (17) was performed within the MATLAB R2011a© environment by adopting the Levenberg–Marquardt algorithm developed for nonlinear least squares fits (Levenberg, 1944; Marquardt, 1963). The uncertainty associated with each estimated value was estimated from the parameter

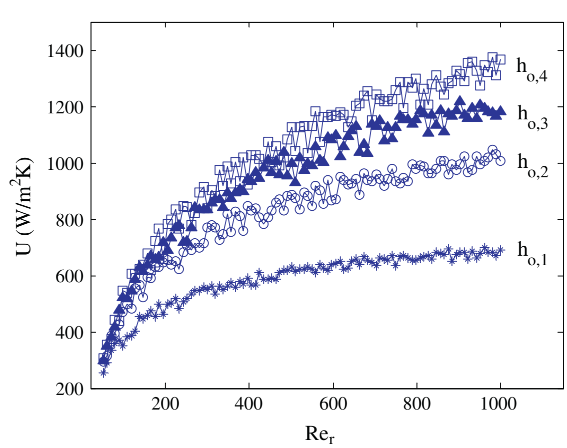

Fig. 3. Synthetic U data sets with σ = 1% for different h_o values.

Table 1
Best estimates and uncertainty analysis for the data set with h_o = 1000 W/m^2 K.

Unknown parameter	Exact value	Estimated alue	$CI^{95\%}$	CV (%)
σ = 1%				
h_o (W/m^2 K)	1000	991	(968, 1014)	1.2
C	1.80	1.80	(1.32, 2.27)	13
α	0.760	0.773	(0.741, 0.803)	2.0
β	0.240	0.233	(0.210, 0.257)	5.2
σ = 5%				
h_o (W/m^2 K)	1000	883	(816, 951)	3.9
C	1.80	0.38	(−0.27, 1.03)	87
α	0.760	0.950	(0.778, 1.211)	9.2
β	0.240	0.335	(0.172, 0.498)	25

Table 2
Best estimates and uncertainty analysis for the data set with h_o = 4000 W/m^2 K.

Unknown parameter	Exact value	Estimated value	$CI^{95\%}$	CV (%)
σ = 1%				
h_o (W/m^2 K)	4000	3991	(3847, 4135)	1.8
C	1.80	1.79	(1.59, 1.97)	5.5
α	0.760	0.762	(0.749, 0.775)	0.87
β	0.240	0.239	(0.230, 0.248)	1.8
σ = 5%				
h_o (W/m^2 K)	4000	3901	(3084, 4718)	11
C	1.80	1.60	(0.52, 2.67)	34
α	0.760	0.778	(0.699, 0.856)	5.1
β	0.240	0.244	(0.190, 0.297)	11

covariance matrix by asymptotic theory (Banks et al., 2010; Seber and Wild, 2003). Both the 95% confidence intervals and the coefficients of variation were calculated, according to Eqs. (14) and (15).

Tables 1 and 2 report the results for the cases h_o = 1000 W/m^2 K and h_o = 4000 W/m^2 K for two different noise levels. As expected from the outcome of the sensitivity analysis, for the lowest value of the external side heat transfer coefficient (h_o = 1000 W/m^2 K), the highest uncertainty is associated with the estimation of the multiplicative constant C and the Prandtl exponent β. For the highest noise level (σ = 5%), the accurate estimation of C becomes practically infeasible (coefficient of variation of 87%). For the same noise level, when the external side heat transfer coefficient is increased (h_o = 4000 W/m^2 K), the estimation of the multiplicative constant C is still critical, although the coefficient of variation decreases to 34%.

One strategy to address the problem of the low sensitivity coefficient of C is to minimise the following functional:

$$S(h_{o,1}, h_{o,2}, \ldots, h_{o,K-1}, h_{o,K}, C, \alpha, \beta) = \sum_{j=1}^{M \cdot K} [U_{\exp,j} - U_{calc,j}]^2 \qquad (18)$$

i.e., by simultaneously assuming that all the parameters K, h_o values, and C, α and β are unknown.

In minimising the objective function in Eq. (18) due to the high number of unknown parameters, it is necessary to verify that the solution algorithm correctly finds the global minimum, avoiding remaining stuck in a local minimum as observed by Pacheco-Vega et al. (2003) for the global regression of heat exchanger data.

Table 3 reports the results of the optimisation problem for the case $K = 4$ (namely, $h_{o,1}$ = 1000, $h_{o,2}$ = 2000, $h_{o,3}$ = 3000 and $h_{o,4}$ = 4000 W/m^2 K) and σ = 1% and σ = 5%. This strategy enabled improving the accuracy of the estimation of C by enhancing the accuracy of the estimation of the other unknown parameters. This improvement is verified for both noise levels.

Table 3
Best estimates and uncertainty analysis for the whole data set (Eq. (18), K = 4).

Unknown parameter	Exact value	Estimated value	$CI^{95\%}$	CV (%)
σ = 1%				
$h_{o,1}$ (W/m^2 K)	1000	996	(987, 1006)	0.48
$h_{o,2}$ (W/m^2 K)	2000	1982	(1948, 2016)	0.87
$h_{o,3}$ (W/m^2 K)	3000	2953	(2879, 3028)	1.3
$h_{o,4}$ (W/m^2 K)	4000	3919	(3790, 4049)	1.7
C	1.80	1.71	(1.54, 1.87)	5.2
α	0.760	0.766	(0.754, 0.778)	0.79
β	0.240	0.243	(0.235, 0.252)	1.7
σ = 5%				
$h_{o,1}$ (W/m^2 K)	1000	971	(928, 1014)	2.2
$h_{o,2}$ (W/m^2 K)	2000	1929	(1777, 2081)	4.0
$h_{o,3}$ (W/m^2 K)	3000	2886	(2553, 3220)	5.9
$h_{o,4}$ (W/m^2 K)	4000	3744	(3186, 4302)	7.6
C	1.80	1.62	(0.808, 2.431)	26
α	0.760	0.788	(0.729, 0.847)	3.8
β	0.240	0.237	(0.195, 0.279)	9.0

Table 4
Best estimates and uncertainty analysis for the data set with h_o = 150 W/m^2 K, σ = 5%.

Unknown parameter	Exact value	Estimated value	$CI^{95\%}$	CV (%)
h_o (W/m^2 K)	150	151	(141, 161)	3.3
C	1.80	0.180	(−0.743, 1.10)	261
α	0.760	0.699	(0.314, 1.08)	28
β	0.240	0.577	(0.0480, 1.11)	47

Table 5
Best estimates and uncertainty analysis for the data set with h_o = 300 W/m^2 K, σ = 5%.

Unknown parameter	Exact value	Estimated value	$CI^{95\%}$	CV (%)
h_o (W/m^{2}K)	300	301	(286, 315)	2.5
C	1.80	2.17	(−0.866, 5.20)	71
α	0.760	0.739	(0.572, 0.905)	12
β	0.240	0.228	(0.0924, 0.364)	30

To verify the effectiveness of this approach for different secondary fluids, a new set of synthetic data was generated considering the convective heat transfer coefficient of the fluid stream flowing in the jacket side over the range of 150–400 W/m^2 K; these values are representative of operating conditions in which a highly viscous liquid, that necessarily flows under the laminar flow regime, is used as the secondary fluid (e.g., diathermic oils). Tables 4 and 5 report the results obtained by separately considering each set of data characterised by a given h_o value for the cases h_o = 150 W/m^2 K and h_o = 300 W/m^2 K, assuming a noise of σ = 5%. As in this case the magnitude of the inner resistance is less than that of the outer side thermal resistance, the estimation of the multiplicative constant C is even more critical than in the previous cases.

Table 6 summarises the results of the optimisation problem based on the assumption that all unknown parameters are simultaneously unknown. The results confirm that this strategy enables an improvement in the accuracy of the estimation of all parameters also in the case of laminar flow conditions in the jacket side.

Table 6
Best estimates and uncertainty analysis for the whole data set (Eq. (18), $K = 4$), $\sigma = 5\%$.

Unknown parameter	Exact value	Estimated value	$CI^{95\%}$	CV (%)
$h_{o,1}$ (W/m^2 K)	150	151	(147, 155)	1.3
$h_{o,2}$ (W/m^2 K)	200	202	(196, 208)	1.5
$h_{o,3}$ (W/m^2 K)	250	253	(244, 262)	1.9
$h_{o,4}$ (W/m^2 K)	300	303	(290, 316)	2.2
C	1.80	2.19	(−0.34, 7.72)	59
α	0.760	0.711	(0.578, 0.843)	9.5
β	0.240	0.241	(0.128, 0.354)	24

4. Application of the parameter estimation approach to experimental data

4.1. Experimental facility

The estimation methodology described above was assessed in an SSHE prototype provided by MBS S.r.l. (Parma–Italy). The product to be heated/cooled flows axially in an annular section between a stationary outer cylinder and a powered coaxial rotor. The inner wall of the outer cylinder is periodically scraped by two couples of alternate blades attached to the rotor. Fig. 4 presents a sketch of the coaxial SSHE, while Fig. 5 shows a sketch of the heat exchanger cross section tested here. The main geometrical characteristics are reported in Table 7. The blades are made of plastic material (Ryton®), while the rotor, stator and external jacket are made of AISI 316L steel.

The rotor is driven by a three phase asynchronous electric motor with a variable speed drive. The working fluid is pure glycerol, and both heating and cooling conditions were tested by adopting hot or cold water as the secondary fluid, flowing in a separate loop. The jacket side contains baffles with a pitch of 200 mm that force the secondary fluid to follow a helical path along the heat exchanger. The product is conveyed by a screw pump from a tank to the heat exchanger. The product flow rate was measured by a volumetric flowmeter (CRAIND, model Kontax) placed upstream of the inlet section of the heat exchanger, while the water stream flow rate was measured by a magnetic flowmeter (SIEMENS, model mag5000).

To simulate a steady state condition, the working fluid was thermally treated in the SSHE and then reconditioned to a fixed temperature in a recovery heat exchanger fed by city water before being delivered to the tank. The hot water was provided by a gas boiler connected to a storage tank, which was thermally insulated from the environment, while the cold water was provided by the tap water loop. A centrifugal pump conveyed the water stream from the tank to the SSHE. Both the working and secondary fluid inlet and outlet bulk temperatures were evaluated by averaging the temperature values acquired by thermocouples placed at three different radial positions on each tube section.

The whole heat exchanger was thermally insulated from the environment by means of a 2 cm Armaflex® layer. All the instruments were connected to an Agilent Technologies multimeter (model 34970A), driven by a personal computer.

The standard approach of Kline and McClintock (1953) was adopted to perform the error analysis: the maximum uncertainty associated with the convective heat transfer coefficient was ±15% (Rainieri et al., 2012b).

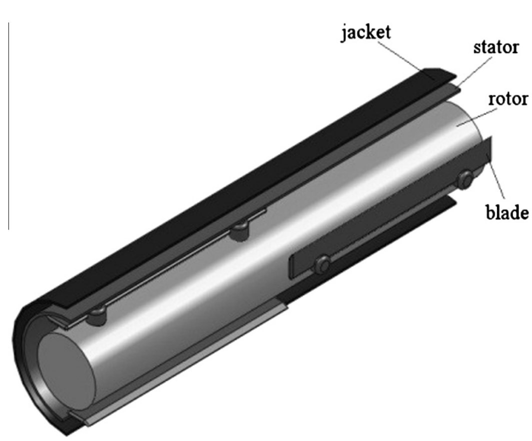

Fig. 4. Sketch of the coaxial alternate blade SSHE used for these experiments.

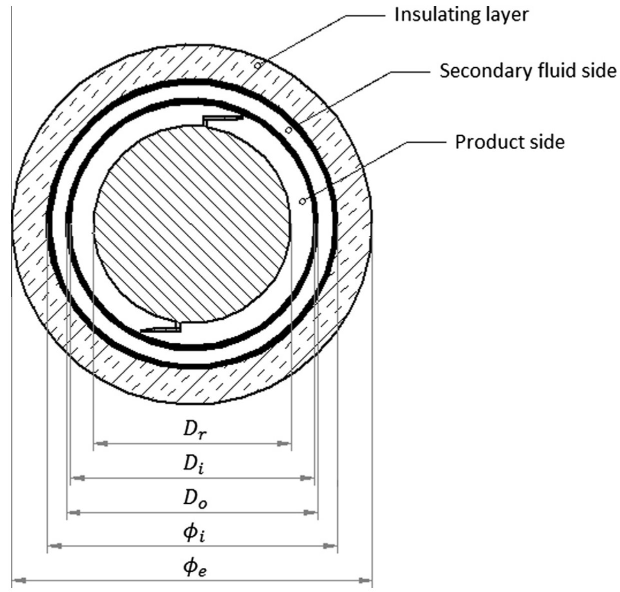

Fig. 5. Cross section of the SSHE.

Table 7
SSHE geometric characteristics.

Symbol	Description	Value (mm)
D_i	Exchanger tube inner diameter	152
D_o	Exchanger tube outer diameter	156
D_r	Rotor shaft diameter	102
L	Tube exchanger length	2000
ϕ_e	Exchanger external diameter	230
ϕ_i	Jacket tube external diameter	188

4.2. Results

To simulate the typical operating conditions of SSHEs in the food industry, which generally handle highly viscous fluids, glycerol was used as the working fluid and water was used as the service fluid. Different sets of runs, each characterised by a constant outer-side water mass flow rate value, were considered by varying the rotor velocity over the range of 0.57–3.5 r.p.s. to emphasise the heat exchanger's behaviour in the laminar and vortical regimes. Table 8 reports the experimental conditions of some representative runs. In the data processing and the definition of the dimensionless parameters, the properties of the working fluid (glycerol) were evaluated at the average bulk temperature between the inlet and outlet sections.

The measured and calculated values of the overall heat transfer coefficient were forced to match by minimising the functional S given by Eq. (18) by adopting the parameter estimation approach described in the previous paragraph.

Table 8
Experimental conditions of some representative runs.

m_o (kg/s)	$T_{o,in}$ (°C)	$T_{o,out}$ (°C)	$T_{i,in}$ (°C)	$T_{i,out}$ (°C)	N (r.p.s.)
Heating conditions					
0.63	63.1	60.7	36.5	41.4	0.57
	62.8	60.2	40.0	46.3	1.17
	62.0	59.2	43.9	50.6	2.2
	62.0	59.3	45.3	51.9	2.83
	62.1	59.4	45.7	52.3	3.08
0.90	62.3	60.6	36.8	41.8	0.57
	62.0	60.1	39.1	45.1	0.92
	61.4	59.3	43.7	50.4	1.75
	61.3	59.2	44.2	50.9	2.00
	61.1	59.0	45.1	51.8	2.50
m_o (kg/s)	$T_{i,in}$ (°C)	$T_{i,out}$ (°C)	$T_{o,in}$ (°C)	$T_{o,out}$ (°C)	N (r.p.s.)
Cooling conditions					
0.61	56.40	44.2	15.0	19.0	0.57
	53.23	40.4	14.8	19.6	1.17
	51.81	38.4	14.9	19.6	1.75
	48.02	34.2	15.2	20.1	3.33
	47.88	33.9	15.0	19.9	3.50
0.89	61.54	47.3	14.4	17.9	0.57
	56.52	40.4	14.4	18.5	1.75
	54.63	38.0	14.4	18.7	2.50
	53.54	36.6	14.4	18.6	3.08
	52.98	35.9	14.4	18.6	3.50

This approach estimated the outer-side convective heat transfer coefficient, assumed to be constant for each water mass flow rate value, the multiplicative constant C and both the rotational Reynolds and Prandtl number exponents.

The assumption of the constant value of the outer side heat transfer coefficient for a given water mass flow rate value is justified by the fact that under the present experimental conditions, the average water temperature varies ±0.5 °C from one run to another (see Table 8), and therefore the thermal properties (density, viscosity, thermal conductivity and specific heat) are expected to change to a limited degree. Under these conditions, h_o is expected to depend mainly on the mean fluid velocity.

A simplified approach was considered for the minimisation procedure: unique values for the exponents of the Prandtl and the rotational Reynolds numbers were considered over the whole rotational velocity range, although different flow regimes are expected to occur in the Re_r range investigated here.

Table 9 reports the results of the optimisation procedure for both the heating and cooling conditions. As predicted by the application of the estimation procedure to the synthetic data, the highest uncertainty is associated with the estimation of the multiplicative constant for both the heating and cooling conditions (coefficient of variation of approximately 30%), while both the Reynolds and Prandtl number exponents are determined with a coefficient of variation of approximately 6%. The experimental data are compared to the optimal correlations found in Figs. 6 and 7; accounting for the experimental error, all the data fall within an error margin of ±20%.

The results obtained here for α ($0.60 < \alpha < 0.77$) for the heating conditions are in good agreement with the data reported for the transitional flow regime in SSHEs by Härröd (1986), who reported values of the exponent of the rotational Reynolds number in the range of 0.6–0.96 under these flow conditions. A slightly lower α value was obtained for the cooling conditions ($0.47 < \alpha < 0.60$). For the Prandtl number exponents, the optimal value found for the heating conditions ($0.16 < \beta < 0.20$) is close to the value predicted by Sykora et al. (1968) ($\beta = 0.24$), while the result for the cooling conditions ($0.37 < \beta < 0.47$) is in good agreement with penetration theory with surface renewal prediction ($\beta = 0.5$), as reported by Higbie (1935) and Kool (1958).

Table 9
Best estimates and uncertainty analysis for the experimental data set (heating and cooling conditions).

Unknown parameter	Estimated value	$CI^{95\%}$	CV (%)
Heating conditions			
$h_{o,1}$ (W/m^2 K)	1527	(1255, 1799)	9.3
$h_{o,2}$ (W/m^2 K)	1690	(1322, 2058)	11
$h_{o,3}$ (W/m^2 K)	2057	(1405, 2708)	16
$h_{o,4}$ (W/m^2 K)	2398	(1400, 3395)	21
C	2.7	(1.3, 4.1)	27
α	0.69	(0.60, 0.77)	6.2
β	0.18	(0.16,0.20)	5.9
Cooling conditions			
$h_{o,1}$ (W/m^2 K)	1844	(1258, 2430)	16
$h_{o,2}$ (W/m^2 K)	2001	(1313, 2689)	18
$h_{o,3}$ (W/m^2 K)	2330	(1397, 3262)	20
$h_{o,4}$ (W/m^2 K)	2425	(1414, 3435)	21
C	0.90	(0.39, 1.40)	29
α	0.54	(0.47, 0.60)	5.9
β	0.42	(0.37, 0.47)	5.8

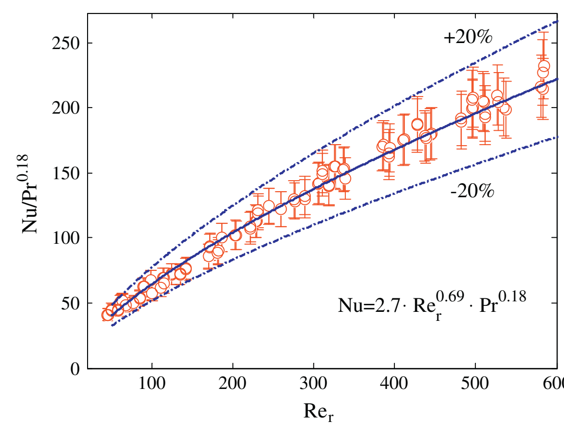

Fig. 6. Optimal Nusselt number correlation for the heating conditions.

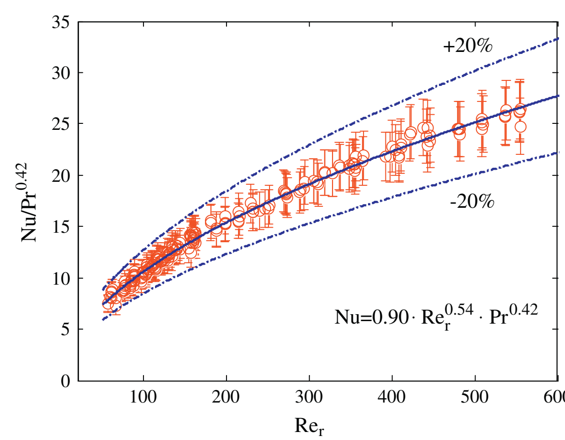

Fig. 7. Optimal Nusselt number correlation for the cooling conditions.

To assess the robustness of the parameter estimation methodology, the restored internal-side Nu data were then compared in more detail with the correlations derived by modifying the penetration theory outcomes as suggested by Härröd (1986). According to this theory, originally formulated by Higbie (1935) and applied to SSHEs by Kool (1958) with limited success, the product Nusselt number correlation is expressed as follows:

$$Nu = 2 \cdot \pi^{-0.5} \cdot (Re_r \cdot Pr \cdot n)^{0.5} \tag{19}$$

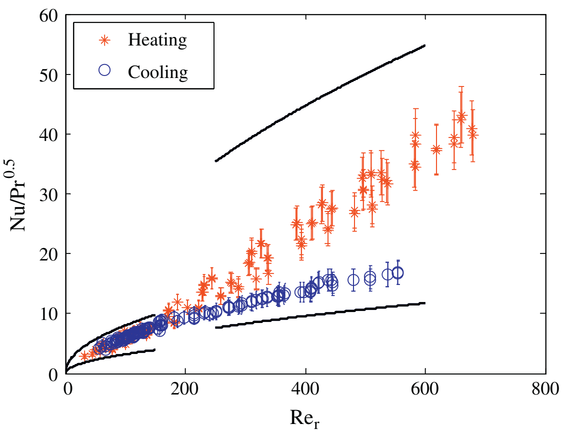

Fig. 8. Comparison between the performance of the SSHE under test and the prediction of the modified penetration theory (continuous line).

where n is the number of blades.

Härröd (1986) analysed the experimental results available in the literature and observed that the product Nusselt number varied from 0.2 to 0.5 and from 0.3 to 1.4 times the value predicted by Eq. (19) for the laminar and vortical flow regimes, respectively. The present experimental data are compared with the predictions of the modified penetration theory under the approach suggested by Härröd (1986) in Fig. 8.

This comparison highlights that the parameter estimation procedure adopted here provided internal side Nu values that are coherent with the data available in the literature for SSHEs. Moreover, this comparison highlights that for Re_r values lower than 250, considered as the critical value for the departure from the laminar flow regime (Härröd, 1986), the thermal performance of the SSHE is similar in heating and cooling conditions. Increasing the Re_r results in lower product Nu data in cooling conditions than in heating conditions. This can be explained by the strong effect of the temperature dependence of the viscosity of the working fluid on the onset of the vortical flow regime.

Note that under the operating conditions investigated here, the inner to outer side thermal resistance ratio was in the range of 0.4–2. Therefore, for the present conditions, neglecting the external side thermal resistance would have led to a misinterpretation of the experimental data.

5. Conclusions

The aim of the present investigation was to enable the robust estimation of the heat transfer correlation for the product side Nusselt number in an SSHE by assuming that the values of the external side heat transfer coefficient are unknown, as well. The estimation procedure presented here did not require any hypothesis about the functional dependence of the external side heat transfer coefficient, as is generally assumed in modified Wilson plot approaches.

The procedure was validated through its application to both synthetic and experimental data acquired from a coaxial alternate blade SSHE pilot plant planned to treat highly viscous fluid foods. The parameter estimation procedure was optimised for sensitivity and uncertainty analysis, which provided considerable insight into the problem.

The application to synthetic data demonstrated that under typical operating conditions, some parameters have areas of insensitivity, especially in the presence of highly noisy data. A strategy was developed to enhance the parameter estimation procedure by simultaneously processing different sets of data characterised by different secondary fluid mass flow rates. The success of the parameter estimation methodology was verified for both the laminar and turbulent flow regimes for the secondary fluid stream heat transfer modality.

The application to the experimental data confirmed that from the measured values of the overall heat transfer coefficient, the secondary fluid heat transfer coefficient, and the power law dependence of the internal fluid Nusselt number on the rotational Reynolds number and the Prandtl number can be successfully estimated together with the multiplicative constant for both the heating and cooling conditions.

The uncertainty analysis provided the confidence intervals associated with each estimated parameter, enabling the quality and robustness of the resulting heat transfer correlation to be assessed.

Regarding the experimental data, the highest uncertainty was associated with the estimation of the multiplicative constant (coefficient of variation of approximately 30%), while both the Reynolds and Prandtl number exponents were determined with a coefficient of variation of approximately 6%.

The methodology presented in this study offers the ability to estimate all the unknown parameters that are crucial for the design and optimisation of SSHEs, which often must be customised to enable specific thermal treatment of highly viscous fluid foods.

Acknowledgments

This work was partially supported by the Emilia-Romagna Region (POR FSE 2007-2013).

MBS S.r.l. is gratefully acknowledged for setting up the experimental apparatus.

The Authors thank Ing. Carlo Corradi and Ing. Marco Mordacci for their support of the experimental work and Prof. Giorgio Pagliarini for helpful and valuable discussions about the results presented here.

References

Abichandani, H., Sarma, S.C., 1987. Hydrodynamics and heat transfer in liquid full scraper surface heat exchanger – a review. Journal of Food Process Engineering 9 (2), 121–141.

Banks, H.T., Holm, K., Robbins, D., 2010. Standard error computations for uncertainty quantification in inverse problems: asymptotic theory vs. bootstrapping. Mathematical and Computer Modelling 52, 1610–1625.

Beck, J.V., Arnold, K.J., 1977. Parameter Estimation in Engineering and Science. John Wiley & Sons, New York.

Boccardi, G., Celata, G.P., Lazzarini, R., Saraceno, L., Trinchieri, R., 2010. Development of a heat transfer correlation for a scraped-surface heat exchanger. Applied Thermal Engineering 30 (10), 1101–1106.

Bozzoli, F., Rainieri, S., Mordacci, M., Pagliarini, G., 2010. Experimental investigation on the heat transfer performance of a scraped surface heat exchanger for highly viscous foods. In: Proc. 14th International Heat Transfer Conference, IHTC, vol. 14(4), pp. 713–718.

Briggs, D.E., Young, E.H., 1969. Modified Wilson plot technique for obtaining heat transfer correlations for shell and tube heat exchangers. Chemical Engineering Progress Symposium Series 65 (92), 35–45.

D'Addio, L., Carotenuto, C., Di Natale, F., Nigro, R., 2012. A new arrangement of blades in scraped surface heat exchangers for food pastes. Journal of Food Engineering 108 (1), 143–149.

D'Addio, L., Carotenuto, C., Di Natale, F., Nigro, R., 2013. Heating and cooling of hazelnut paste in alternate blades scraped surface heat exchangers. Journal of Food Engineering 115 (2), 182–189.

Datta, A.K., 2002. Biological and Bioenvironmental Heat and Mass Transfer. Marcel Dekker, Inc., New York–Basel.

Fayolle, F., Belhamri, R., Flick, D., 2013. Residence time distribution measurements and simulation of the flow pattern in a scraped surface heat exchanger during crystallisation of ice cream. Journal of Food Engineering 116 (2), 390–397.

Fernández-Seara, J., Uhía, F.J., Sieres, J., Campo, A., 2007. A general review of the Wilson plot method and its modifications to determine convection coefficients in heat exchange devices. Applied Thermal Engineering 27 (17–18), 2745–2757.

Geankoplis, C.J., 2003. Transport Processes and Separation Process Principles. Prentice Hall Ed., Upper Saddle River, NJ.

Härröd, M., 1986. Hydrodynamics scraped surface heat exchangers. Journal of Food Process Engineering 9, 1–62.

Higbie, R., 1935. The rate of the absorption of a pure gas into a still liquid during short periods of exposure. Transactions of the American Institute of Chemical Engineers 31, 365–389.

Khartabil, H.F., Christensen, R.N., 1992. An improved scheme for determining heat transfer correlations from heat exchanger regression models with three unknowns. Experimental Thermal and Fluid Science 5, 808–819.

Kline, S.J., McClintock, F.A., 1953. Describing uncertainties in single-sample experiments. Mechanical Engineering 75.

Kool, J., 1958. Heat transfer in scraped vessels and pipes handling viscous materials. Transactions of the Institution of Chemical Engineers 36a, 253–258.

Levenberg, K., 1944. A method for the solution of certain non-linear problems in least squares. The Quarterly of Applied Mathematics 2, 164–168.

Marquardt, D.W., 1963. An algorithm for least-squares estimation of nonlinear parameters. Journal of the Society for Industrial and Applied Mathematics 11 (2), 431–441.

Pacheco-Vega, A., Sen, M., Yan, K.T., 2003. Simultaneous determination of in- and over-tube heat transfer correlations in heat exchangers by global regression. International Journal of Heat and Mass Transfer 46 (6), 1029–1040.

Rainieri, S., Bozzoli, F., Schiavi, L., Pagliarini, G., 2011. Numerical analysis of convective heat transfer enhancement in swirl tubes. International Journal of Numerical Methods for Heat and Fluid Flow 21 (5), 559–571.

Rainieri, S., Bozzoli, F., Pagliarini, G., 2012a. Experimental investigation on the convective heat transfer in straight and coiled corrugated tubes for highly viscous fluids: preliminary results. International Journal of Heat and Mass Transfer 55 (1–3), 498–504.

Rainieri, S., Bozzoli, F., Mordacci, M., Pagliarini, G., 2012b. Numerical 2-D modeling of a coaxial scraped surface heat exchanger versus experimental results under the laminar flow regime. Heat Transfer Engineering 33 (13), 1120–1129.

Rainieri, S., Bozzoli, F., Cattani, L., Pagliarini, G., 2013. Compound convective heat transfer enhancement in helically coiled wall corrugated tubes. International Journal of Heat and Mass Transfer 59 (1), 353–362.

Rose, J.W., 2004. Heat-transfer coefficients, Wilson plots and accuracy of thermal measurements. Experimental Thermal and Fluid Sciences 28 (2–3), 77–86.

Rozzi, S., Massini, R., Paciello, G., Pagliarini, G., Rainieri, S., Trifirò, A., 2007. Heat treatment of fluid foods in a shell and tube heat exchanger: comparison between smooth and helically corrugated wall tubes. Journal of Food Engineering 79 (1), 249–254.

Seber, G.A.F., Wild, C.J., 2003. Nonlinear Regression. Wiley-Interscience, Hoboken, NJ.

Skelland, A.H.P., 1958. Correlation of scraped-film heat transfer in the votator. Chemical Engineering Science 7 (3), 166–175.

Styrylska, T.B., Lechowska, A.A., 2003. Unified Wilson plot method for determining heat transfer correlations for heat exchangers. Journal of Heat Transfer – Transactions of the ASME 25, 752–756.

Sykora, S., Navratil, B., Karasek., O., 1968. Heat transfer on scraped walls in the laminar and transitional regions. Collection of Czechoslovak Chemical Communications 33 (2), 518–528.

Uhia, F.J., Campo, A., Fernandez-Seara, J., 2013. Uncertainty analysis for experimental heat transfer data obtained by the Wilson plot method: application to condensation on horizontal plain tubes. Thermal Science 17 (2), 471–487.

Wilson, E.E., 1915. A basis of rational design of heat transfer apparatus. ASME Journal of Heat Transfer 37, 47–70.

Yataghene, M., Legrand, J., 2013. A 3D-CFD model thermal analysis within a scraped surface heat exchanger. Computers & Fluids 71, 380–399.